DIPHOTON SPECTRUM IN THE MASS RANGE 120-140 GEV AT THE LHC

L.J CIERI
INFN, Sezione di Firenze, Via Sansone 1, I-50019 Sesto Fiorentino, Florence, Italy

We consider direct diphoton production in hadron collisions. We compute the next-to-next-to-leading order (NNLO) QCD radiative corrections at the fully-differential level. Our calculation uses the q_T subtraction formalism and it is implemented in a parton level Monte Carlo program, which allows the user to apply arbitrary kinematical cuts on the final-state photons and the associated jet activity, and to compute the corresponding distributions in the form of bin histograms. We present selected numerical results related to Higgs boson searches at the LHC, and we show how the NNLO corrections to diphoton production are relevant to understand the main background of the decay channel $H \to \gamma\gamma$.

1 Introduction

Diphoton production is a relevant process in hadron collider physics. It is both a classical signal within the Standard Model (SM) and an important background for Higgs boson and new-physics searches. Recent results from the LHC indicates that the Higgs boson mass m_H must be low (114 GeV$< m_H <$ 130 GeV), and thus the preferred search mode involves Higgs boson production via gluon fusion followed by the rare decay into a pair of photons. We are interested in the process $pp \to \gamma\gamma X$, which, at the lowest order in perturbative QCD, occurs *via* the quark annihilation subprocess $q\bar{q} \to \gamma\gamma$. The QCD corrections at the next-to-leading order (NLO) in the strong coupling α_S involve the quark annihilation channel and a new partonic channel, *via* the subprocess $qg \to \gamma\gamma q$. These corrections have been computed and implemented in the fully-differential Monte Carlo codes `DIPHOX`,[1] `2gammaMC` [2] and `MCFM`.[3] A calculation that includes the effects of transverse-momentum resummation is implemented in `RESBOS`.[4] At the next-to-next-to-leading order (NNLO), the gg channel starts to contribute, and the large gluon–gluon luminosity makes this channel sizeable. Part of the contribution from this channel, the so called *box contribution*, was computed long ago[5] and its size turns out to be comparable to the lowest-order result. Besides their *direct* production from the hard subprocess, photons can also arise from fragmentation subprocesses of QCD partons. The computation of fragmentation subprocesses requires (poorly known) non-perturbative information, in the form of parton fragmentation functions of the photon. The complete NLO single- and double-fragmentation contributions are implemented in `DIPHOX`.[1] The effect of the fragmentation contributions is sizeably reduced by the photon isolation criteria that are necessarily applied in hadron collider experiments to suppress the very large irreducible background (e.g., photons that are faked by jets or produced by hadron decays). The standard cone isolation and the 'smooth' cone isolation proposed by Frixione [6] are two of these criteria. The standard cone isolation is easily implemented in experiments, but it only suppresses a fraction of the fragmentation contribution. The smooth cone isolation (formally) eliminates the entire fragmentation contribution, but its experimental implementation

is still under study.[7] However, it is important to anticipate (work to appear), that in some kinematical regions (e.g for Higgs boson searches), the standard cone and the Frixione isolation criteria give basically the same theoretical answer.[a]

2 Diphoton production at NNLO

We consider the inclusive hard-scattering reaction $h_1 + h_2 \to \gamma\gamma + X$, where the collision of the two hadrons, h_1 and h_2, produces the diphoton system $F \equiv \gamma\gamma$ with high invariant mass $M_{\gamma\gamma}$. The evaluation of the NNLO corrections to the this process requires the knowledge of the corresponding partonic scattering amplitudes with $X = 2$ partons (at the tree level, [8]) $X = 1$ parton (up to the one-loop level [9]) and no additional parton (up to the two-loop level [10]) in the final state. The implementation of the separate scattering amplitudes in a complete NNLO (numerical) calculation is severely complicated by the presence of infrared (IR) divergences that occur at intermediate stages. The q_T subtraction formalism [11] is a method that handles and cancels these unphysical IR divergences up to the NNLO. The formalism applies to generic hadron collision processes that involve hard-scattering production of a colourless high-mass system F. Within that framework,[11] the corresponding cross section is written as:

$$d\sigma^F_{(N)NLO} = \mathcal{H}^F_{(N)NLO} \otimes d\sigma^F_{LO} + \left[d\sigma^{F+\text{jets}}_{(N)LO} - d\sigma^{CT}_{(N)LO} \right] \quad , \tag{1}$$

where $d\sigma^{F+\text{jets}}_{(N)LO}$ represents the cross section for the production of the system F plus jets at (N)LO accuracy [b], and $d\sigma^{CT}_{(N)LO}$ is a (IR subtraction) counterterm whose explicit expression [13] is obtained from the resummation program of the logarithmically-enhanced contributions to q_T distributions. The 'coefficient' $\mathcal{H}^F_{(N)NLO}$, which also compensates for the subtraction of $d\sigma^{CT}_{(N)LO}$, corresponds to the (N)NLO truncation of the process-dependent perturbative function

$$\mathcal{H}^F = 1 + \frac{\alpha_S}{\pi}\,\mathcal{H}^{F(1)} + \left(\frac{\alpha_S}{\pi}\right)^2 \mathcal{H}^{F(2)} + \dots \quad . \tag{2}$$

The NLO calculation of $d\sigma^F$ requires the knowledge of $\mathcal{H}^{F(1)}$, and the NNLO calculation also requires $\mathcal{H}^{F(2)}$. The general structure of $\mathcal{H}^{F(1)}$ is explicitly known;[14] exploiting the explicit results of $\mathcal{H}^{F(2)}$ for Higgs [11,15] and vector boson [16] production we have generalized the process-independent relation of Ref.[14] to the calculation of the NNLO coefficient $\mathcal{H}^{F(2)}$.

3 Quantitative results

We have performed our fully-differential NNLO calculation [17] of diphoton production according to Eq. (1). The NNLO computation is encoded in a parton level Monte Carlo program, in which we can implement arbitrary IR safe cuts on the final-state photons and the associated jet activity. We concentrate on the direct production of diphotons, and we rely on the smooth cone isolation criterion.[6] Considering a cone of radius $r = \sqrt{(\Delta\eta)^2 + (\Delta\phi)^2}$ around each photon, we require the total amount of hadronic (partonic) transverse energy E_T inside the cone to be smaller than $E_{T\,max}(r)$,

$$E_T < E_{T\,max}(r) \equiv \epsilon_\gamma\, p_T^\gamma \left(\frac{1-\cos r}{1-\cos R}\right)^n \quad , \tag{3}$$

where p_T^γ is the photon transverse momentum; the isolation criterion $E_T < E_{T\,max}(r)$ has to be fulfilled for all cones with $r \le R$. We use the MSTW 2008 [18] sets of parton distributions,

[a] The use of the same parameters in both criteria is understood.

[b] In the case of diphoton production, the NLO calculation of $d\sigma^{\gamma\gamma+\text{jets}}_{NLO}$ was performed in Ref.[12]

with densities and α_S evaluated at each corresponding order, and we consider $N_f = 5$ massless quarks/antiquarks and gluons in the initial state. The default renormalization (μ_R) and factorization (μ_F) scales are set to the value of the invariant mass of the diphoton system, $\mu_R = \mu_F = M_{\gamma\gamma}$. The QED coupling constant α is fixed to $\alpha = 1/137$.

To present some quantitative results, we consider diphoton production at the LHC ($\sqrt{s} =$

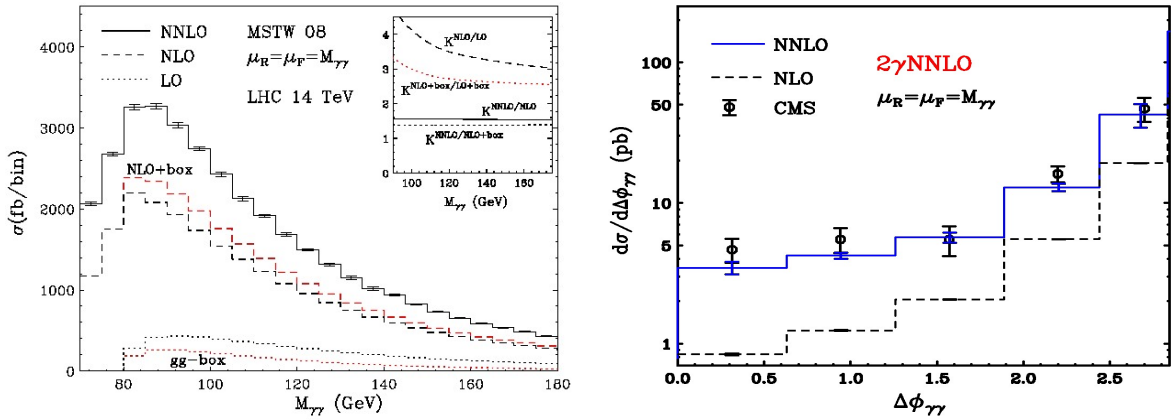

Figure 1: *Left: Invariant mass distribution of the photon pair at the LHC ($\sqrt{s} = 14$ TeV): LO (dots), NLO (dashes) and NNLO (solid) results. We also present the results of the box and NLO+box contributions. The inset plot shows the corresponding* K*-factors. Right: Diphoton cross section as a function of the azimuthal separation of the two photons. Data from CMS*[19] *($\sqrt{s} = 7$ TeV) are compared to the NNLO calculation.*[17]

14 TeV). We apply typical kinematical cuts used by ATLAS and CMS Collaborations in their Higgs search studies. We require the harder and the softer photon to have transverse momenta $p_T^{\rm harder} \geq 40$ GeV and $p_T^{\rm softer} \geq 25$ GeV, respectively. The rapidity of both photons is restricted to $|y_\gamma| \leq 2.5$, and the invariant mass of the diphoton system is constrained to lie in the range $20\,{\rm GeV} \leq M_{\gamma\gamma} \leq 250\,{\rm GeV}$. The isolation parameters are set to the values $\epsilon_\gamma = 0.5$, $n = 1$ and $R = 0.4$. We observe [17] that the value of the cross section remarkably increases with the perturbative order of the calculation. This increase is mostly due to the use of *very asymmetric* (unbalanced) cuts on the photon transverse momenta. At the LO, kinematics implies that the two photons are produced with equal transverse momentum and, thus, both photons should have $p_T^\gamma \geq 40$ GeV. At higher orders, the final-state radiation of additional partons opens a new region of the phase space, where 40 GeV $\geq p_T^{\rm softer} \geq 25$ GeV. Since photons can copiously be produced with small transverse momentum,[17] the cross section receives a sizeable contribution from the enlarged phase space region. This effect is further enhanced by the opening of a new large-luminosity partonic channel at each subsequent perturbative order. In Fig. 1 (left) we compare the LO, NLO and NNLO invariant mass distributions at the default scales. The inset plot shows the K-factors defined as the ratio of the cross sections at two subsequent perturbative orders. We note that $K^{NNLO/NLO}$ is sensibly smaller than $K^{NLO/LO}$, and this fact indicates an improvement in the convergence of the perturbative expansion. We find that about 30% of the NNLO corrections is due to the gg channel (the *box contribution* is responsible for more than half of it), while almost 60% still arises from the next-order corrections to the qg channel.

Recent results from the LHC [19,20] and the Tevatron [21] show some discrepancies between the data and NLO theoretical calculations of diphoton production. Basically, discrepancies were found in kinematical regions where the NLO calculation is *effectively* a LO theoretical description of the process. Such phase space regions[c] are accesible at NLO for the first time, due to the

[c] Away from the back-to-back configuration.

final-state radiation of the additional parton.[d] Figure 1 (right) shows a measurement by CMS,[19] of the diphoton cross section as a function of the azimuthal angle $\Delta\phi_{\gamma\gamma}$ between the photons. The data are compared with our NLO and NNLO calculations.[17] The acceptance criteria used in this analysis ($\sqrt{s} = 7$ TeV) require of: $p_T^{\rm harder} \geq 23$ GeV and $p_T^{\rm softer} \geq 20$ GeV. The rapidity of both photons is restricted to $|y_\gamma| \leq 2.5$, and the invariant mass of the diphoton system is constrained to be $M_{\gamma\gamma} > 80\,\text{GeV}$. The isolation parameters are set to the values $\epsilon_\gamma = 0.05$, $n = 1$ and $R = 0.4$. We note that the CMS data are selected by using the standard cone isolation criterion and the constraint in Eq. (3) is applied only to the cone of radius $r = R$. Since the smooth isolation criterion used in our calculation (we apply Eq. (3) for all cones with $r \leq R$) is stronger than the photon isolation used by CMS, we remark that our NLO and NNLO results cannot overestimate the corresponding theoretical results for the CMS isolation criterion. The histograms in Fig. 1 (right) show that the NNLO QCD results remarkably improve the theoretical description of the CMS data throughout the entire range of $\Delta\phi_{\gamma\gamma}$.

The results illustrated in this contribution show that the NNLO description of diphoton production is essential to understand the phenomenology associated to this process, and therefore, the NNLO calculation is a relevant tool to describe the main background for Higgs boson searches.

References

1. T. Binoth, J. P. Guillet, E. Pilon and M. Werlen, Eur. Phys. J. **C16**, 311 (2000).
2. Z. Bern, L. J. Dixon and C. Schmidt, Phys. Rev. **D66**, 074018 (2002).
3. J. M. Campbell, R. K. Ellis and C. Williams, JHEP **1107**, 018 (2011).
4. C. Balazs, E. L. Berger, P. M. Nadolsky and C. -P. Yuan, Phys. Rev. **D76**, 013009 (2007).
5. D. A. Dicus and S. S. D. Willenbrock, Phys. Rev. **D37**, 1801 (1988).
6. S. Frixione, Phys. Lett. **B429**, 369 (1998).
7. R. Blair, B. Brelier, F. Bucci, S. Chekanov, M. Stockton and M. Tripiana, CERN-OPEN-2011-041, (2011).
8. V. D. Barger, T. Han, J. Ohnemus and D. Zeppenfeld, Phys. Rev. **D41**, 2782 (1990); V. Del Duca, W. B. Kilgore and F. Maltoni, Nucl. Phys. **B566**, 252 (2000).
9. Z. Bern, L. J. Dixon and D. A. Kosower, Nucl. Phys. **B437**, 259 (1995); A. Signer, Phys. Lett. **B357**, 204 (1995).
10. C. Anastasiou, E. W. N. Glover and M. E. Tejeda-Yeomans, Nucl. Phys. **B629**, 255 (2002).
11. S. Catani and M. Grazzini, Phys. Rev. Lett. **98**, 222002 (2007).
12. V. Del Duca, F. Maltoni, Z. Nagy and Z. Trocsanyi, JHEP **0304**, 059 (2003).
13. G. Bozzi, S. Catani, D. de Florian and M. Grazzini, Nucl. Phys. **B737**, 73 (2006).
14. D. de Florian and M. Grazzini, Phys. Rev. Lett. **85**, 4678 (2000), Nucl. Phys. **B616**, 247 (2001).
15. S. Catani and M. Grazzini, report ZU-TH-12-11 (arXiv:1106.4652 [hep-ph]).
16. S. Catani, L. Cieri, G. Ferrera, D. de Florian and M. Grazzini, Phys. Rev. Lett. **103**, 082001 (2009).
17. S. Catani, L. Cieri, D. de Florian, G. Ferrera and M. Grazzini, Phys. Rev. Lett. **108** (2012) 072001.
18. A. D. Martin, W. J. Stirling, R. S. Thorne and G. Watt, Eur. Phys. J. **C63**, 189 (2009).
19. S. Chatrchyan *et al.* [CMS Collaboration], arXiv:1110.6461 [hep-ex].
20. G. Aad *et al.* [ATLAS Collaboration], Phys. Rev. D **85** (2012) 012003.
21. T. Aaltonen *et al.* [CDF Collaboration], Phys. Rev. D **84** (2011) 052006.

[d] The low-mass region ($M_{\gamma\gamma} \leq 80 GeV$) in Figure 1 also belongs to this case.